BIOCHEMISTRY
including biophysical chemistry & molecular biology
Article

Biochemistry **2010,** *49,* 9241–9248 9241
DOI: 10.1021/bi1009985

Reduction Kinetics of a Flavin Oxidoreductase LuxG from *Photobacterium leiognathi* (TH1): Half-Sites Reactivity[†]

Sarayut Nijvipakul,[‡] David P. Ballou,*[,§] and Pimchai Chaiyen*[,‡]

[‡]*Department of Biochemistry and Center of Excellence in Protein Structure and Function, Faculty of Science, Mahidol University, Bangkok 10400, Thailand, and* [§]*Department of Biological Chemistry, Medical School, University of Michigan, Ann Arbor, Michigan 48109*

Received June 21, 2010; Revised Manuscript Received August 23, 2010

ABSTRACT: Bacterial bioluminescence is a phenomenon resulting from the reaction of a two-component FMN-dependent aldehyde monooxygenase system, which comprises a bacterial luciferase and a flavin reductase. Bacterial luciferase (LuxAB) is one of the most extensively investigated two-component monooxygenases, while its reductase partner, the flavin reductase (LuxG) from the same operon, has only been recently expressed in a functional form. This work reports transient kinetics identification of intermediates in the LuxG reaction using stopped-flow spectrophotometry. The results indicate that the overall reaction follows a sequential-ordered mechanism in which NADH binds first to the enzyme, followed by FMN, resulting in the formation of charge-transfer intermediate 1 (CT-1) typical of those between reduced pyridine nucleotides and oxidized flavins. The next step is the reduction of FMN as indicated by a large decrease in absorbance at 450 nm. The reduction of FMN is biphasic. The first phase of FMN reduction occurs concurrently with formation of charge-transfer intermediate 2 (CT-2), while the second phase is synchronous with the decay of CT-2. When the isotope-labeled substrate, 4(*R*)-[^{2}H]NADH, was used, the first reduction phase showed a primary kinetic isotope effect ($^{D}k_{red}$) of ≥3.9 and resulted in greater accumulation of CT-1. These results are consistent with CT-1 being the FMN_{ox}:NADH complex, while CT-2 is the FMN_{red}:NAD^+ complex. Because CT-2 decays with a rate constant of $2.8 \pm 0.2\ s^{-1}$, while the turnover number obtained from the steady−steady-state kinetics is $1.7\ s^{-1}$, it is likely that the CT-2 decay step largely controls the overall reaction rate. All kinetic data are consistent with a half-sites reactivity model in which flavin reduction occurs at only one subunit at a time. The first reduction phase is due to the reduction of FMN in the first subunit, while the second phase is due to the reduction of FMN in the second subunit. The latter phase is limited by the rate of decay of CT-2 in the first subunit. The half-sites reactivity model is also supported by detection of burst kinetics during the pre-steady-state period that is correlated with 0.5 mol of the FMN being reduced/mol of the LuxG:NADH complex. The functional importance of this half-site reactivity phenomenon is still unclear.

Flavins (FAD, FMN,[1] and riboflavin), the redox cofactors in flavoproteins, usually participate in catalysis by alternating between oxidized and reduced forms. Because of the tendency of reduced flavins to react with oxygen, most flavoenzymes are found with their flavins in the oxidized form in the resting state, whereas reduced flavins mainly occur as transient intermediates. Nevertheless, reduced flavins have been increasingly found to participate as substrates in a wide variety of biological redox reactions. In prokaryotes, reduced flavins participate in key steps of iron uptake and metabolism (*1*) and activation processes of some enzymes, e.g., chorismate synthase (*2*) and ribonucleotide reductase (*3*). In two-component flavoprotein monooxygenases, reduced flavins are generally reduced by an NAD(P)H reductase component and serve as substrates for an oxygenase component (*4*−*6*). Two-component enzymes are involved in the oxygenation of phenolic compounds (*7*, *8*), the biosynthesis of antibiotics (*9*), and bacterial bioluminescence (*10*−*12*).

In the bacterial luciferase system, the reduced FMN that is required as a substrate is provided by a flavin reductase (*10*, *11*). Although many types of flavin reductases in luminous bacteria have been reported, the only flavin reductases extensively studied are Frase I from *Vibrio fischeri* (*13*) and FRP from *Vibrio harveyi* (*14*). Both enzymes have molecular masses of ∼26 kDa, contain FMN as cofactors, and are classified as members of the class II flavin reductase family (*15*). However, these two reductases have different specificities toward pyridine nucleotides; Frase I can utilize either NADH or NADPH while FRP is specific for NADPH (*13*, *14*). Despite a relatively low sequence identity between these two reductases (10% identity), their three-dimensional folding patterns are very similar (*16*). Unlike the enzymes from *Vibrio* genera, flavin reductases from *Photobacterium* sp. have not been investigated in detail.

[†]This study was supported by The Thailand Research Fund through Grants BRG5180002 (to P.C.) and PHD/0211/2546 of the Royal Golden Jubilee Ph.D. program (to S.N.), by the Faculty of Science, Mahidol University (to P.C.), and by Grant GM64711 from the National Institutes of Health (to D.P.B.). S.N. also received support from Medical Scholars Program, Mahidol University.

*To whom correspondence should be addressed. P.C.: tel, 662-201-5596; fax, 662-354-7174; e-mail, scpcy@mahidol.ac.th. D.P.B.: tel, 734-764-9582; fax, 734-764-3509; e-mail, dballou@umich.edu.

[1]Abbreviations: LuxG, NADH:flavin oxidoreductase from luminous bacteria; FNR, ferredoxin−$NADP^+$ reductase; PDR, phthalate dioxygenase reductase; LuxAB, bacterial luciferase; NADH, reduced nicotinamide adenine dinucleotide; NADD, deuterated 4(*R*)-[^{2}H]NADH; NAD^+, oxidized nicotinamide adenine dinucleotide; FMN, oxidized flavin mononucleotide; $FMNH^-$, reduced flavin mononucleotide; PDO, protocatechuate dioxygenase; PCA, protocatechuate.

Published on Web 09/13/2010

Table 1: Steady-State Kinetic Parameters and Microscopic Rate Constants of LuxG Reaction[a]

kinetic parameter	value
K_M[b]	2.7 μM (for FMN), 15 μM (for NADH)
k_{cat}[b]	1.7 s^{-1}
k_{on}	5.1 × 10^4 M^{-1} s^{-1}
k_{off}	1.3 s^{-1}
K_d (k_{off}/k_{on})	25 ± 2 μM
K_d[c]	25 ± 4 μM
$k_{2(apparent)}$	93 ± 6 s^{-1}
k_3^{NADH}	68 ± 6 s^{-1}
k_3^{NADD}	17.5 s^{-1}
k_4^{NADH}	2.8 ± 0.2 s^{-1}
k_4^{NADD}	2.6 ± 0.2 s^{-1}

[a]Experiments were performed at 4 °C. [b]Rate constants taken from the previous report (*10*). [c]Measured by fluorescence changes on binding (Figure 1C).

LuxG, a novel flavin reductase from *Photobacterium leiognathi*, has recently been cloned and expressed in a functional form by our group. The enzyme has been shown to be a class I flavin reductase that does not bind flavin as a prosthetic group (*10*). A prototype enzyme in this group, *Escherichia coli* Fre, was extensively characterized in terms of structural and kinetic aspects (*17*, *18*). Steady-state kinetic data (Table 1) show that LuxG catalyzes the reaction according to a ternary complex model, similar to the reaction of *E. coli* Fre, although LuxG only shares 37% sequence identity to Fre (*10*). The two enzymes also differ in biochemical properties such as the oligomerization state and substrate specificity. LuxG is a dimer and prefers NADH as a substrate, while Fre is a monomer and uses NADH and NADPH equally well (*10*, *15*, *19*). Phylogenetic analysis, using amino acid sequence data, also shows that LuxGs from various species of luminous bacteria clearly belong to a different subgroup from the Fre subgroup (*20*).

We report here the reduction kinetics of *P. leiognathi* LuxG investigated using stopped-flow spectrophotometry. Transient kinetics shows biphasic flavin reduction and detection of two transient intermediates (the charge-transfer complexes 1 and 2). Primary kinetic isotope effects using 4(*R*)-[^{2}H]NADH were employed to identify hydride transfer steps. Burst kinetic data were used to determine the amount of FMN reduced during the pre-steady-state period prior to steady-state turnovers. Based on these results, a kinetic mechanism for the LuxG reaction was constructed. This is the first detailed report for the reduction kinetics of a functional flavin reductase encoded in the same operon as a bacterial luciferase and from *Photobacterium* sp.

MATERIALS AND METHODS

Reagents. LuxG with a C-terminal His_6 tag was prepared according to protocols in ref *10*. FMN was synthesized by converting FAD to FMN using snake venom from *Crotalus adamanteus* (*21*). NADH was purchased from Sigma. 4(*R*)-NADD was synthesized according to the procedure described by Gassner et al. (*22*) with slight modifications. In brief, yeast alcohol dehydrogenase (0.2 mg) (Sigma) and NAD^+ (25 mg) (Sigma) were combined in 5 mL of 0.1 M NH_4HCO_3 buffer (pH 8.0) containing 0.3 mL of CD_3CD_2OD (Sigma) and incubated at 37 °C. The formation of 4(*R*)-NADD was monitored by measuring the absorbance at 340 nm. After the reaction was complete (by 15 min), the alcohol dehydrogenase was removed by ultrafiltration using Centricon-10 concentrators (Millipore). The filtrate was diluted 5-fold by adding distilled H_2O and applied onto a 5 × 1.5 cm fast-flow DEAE-Sepharose column (GE Healthcare) preequilibrated with water. NADD was eluted about midway through a 300 mL gradient of 0−0.2 M NH_4HCO_3, pH 8.0. Fractions containing NADD and with $A_{260}/A_{340} \leq 2.6$ were combined. The purified NADD was validated by NMR spectroscopy and lyophilized to obtain dry powder and stored at −20 °C until used. Concentrations of the following compounds were determined using the known molar extinction coefficients: NADH and NADD, ε_{340} = 6220 M^{-1} cm^{-1}; NAD^+, ε_{260} = 17800 M^{-1} cm^{-1}; FAD, ε_{450} = 11300 M^{-1} cm^{-1}; FMN, ε_{450} = 12200 M^{-1} cm^{-1}.

Spectroscopic Studies. UV−visible absorbance spectra were recorded with a Hewlett-Packard diode array spectrophotometer (HP8453A), a Shimadzu 2501PC, or a Cary 300Bio spectrophotometer. Fluorescence measurements were carried out with a Shimadzu RF5301PC spectrofluorometer. All spectroscopic instruments were equipped with thermostated cell compartments.

Rapid Kinetic Experiments. Reactions were carried out at 4 °C in 50 mM Tris-HCl buffer, pH 8.0, in the presence of 1 mM DTT and 10% glycerol, unless otherwise specified. Rapid kinetics measurements were performed with a TgK Scientific Model SF-61DX stopped-flow spectrophotometer using both absorbance and fluorescence modes. The optical path length of the observation cell was 1 cm. The stopped-flow apparatus was made anaerobic by flushing the flow system with an anaerobic buffer solution containing protocatechuate (PCA) and protocatechuate dioxygenase (PCD) (*23*). This solution was composed of 400 μM PCA and 1 μM PCD in 50 mM potassium phosphate buffer, pH 7.0. The buffer was made anaerobic by equilibrating with oxygen-free argon that had been passed through an Oxyclear oxygen removal column (Labclear) using an anaerobic train or by equilibrating in the atmosphere of an anaerobic glovebox (Bell Technology) that maintains the level of oxygen lower than 5 ppm. The PCA/PCD solution was allowed to stand in the flow system overnight. The flow unit was rinsed with anaerobic buffer before experiments. Enzyme solutions were made anaerobic in a tonometer by repeated cycles of evacuation and equilibration with oxygen-free argon or prepared in the anaerobic glovebox. Substrate solutions were made anaerobic by bubbling with oxygen-free argon for at least 10 min. Apparent rate constants (k_{obs}) from kinetic traces were calculated from exponential fits using KinetAsyst3 software, Kinetics Studio (TgK Scientific, U.K.), or Program A (written at the University of Michigan by Rong Chang, Jung-yen Chiu, Joel Dinverno, and D. P. Ballou). Rapid kinetic data were plotted for display using the KaleidaGraph software (Synergy). Conditions used during individual experiments are specified in the corresponding figure legends.

Binding of FMN to LuxG. Various concentrations of LuxG (0, 8, 16, 40, and 160 μM) were mixed with 8 μM FMN in 50 mM Tris-HCl buffer, 1 mM DTT, and 10% (v/v) glycerol, pH 8.0, in a final volume of 10 mL. At equilibrium, the bound and free FMN fractions were separated using an ultrafiltration device (Centriprep YM-10; Millipore). The centripreps were centrifuged at 3000 rpm, 4 °C, for 5 min to obtain filtrates of ~800 μL. The filtrate and retentate were analyzed for the amount of free and bound FMN.

Burst Kinetics of the FMN Reduction. Experiments monitoring burst kinetics of FMN reduction in the LuxG reaction were performed in 50 mM Tris-HCl buffer, 10% glycerol, and 1 mM DTT, pH 8.0 at 4 °C, using the stopped-flow apparatus. Anaerobic tonometers containing LuxG at 20, 30, and 40 μM and

NADH at 300 μM (after mixing) were loaded onto one side of the stopped-flow apparatus. The second side contained FMN (120 μM after mixing) in the same buffer. The solutions in both sides were mixed using the stopped-flow apparatus, and the reduction of FMN was monitored by the absorbance change at 450 nm. The data were fit to eq 1 to obtain the parameters at different molar ratios of FMN to the LuxG:NADH complex.

$$A = A_0 e^{-k_{red}t} - v_{ss}(\varepsilon_{450}^{ox \rightarrow red})t + c \quad (1)$$

In eq 1, A is the observed absorbance at 450 nm at time t, A_0 is the absorbance change in the burst due to reduction of FMN (via $k_{red} = 68\ s^{-1}$), v_{ss} is the steady-state turnover rate under these conditions, and c compensates for the nonzero baseline. $\varepsilon_{450}^{ox \rightarrow red}$ is the millimolar absorption coefficient at 450 nm (10.5 mM^{-1} cm^{-1}) for reduction of oxidized to reduced FMN. The value of the burst, $A_0/\varepsilon_{450}^{ox \rightarrow red}$, corresponds to the concentration of flavin being reduced during the first turnover prior to the steady-state phase.

RESULTS

Binding of NADH to LuxG. The kinetics of binding of NADH to LuxG were measured by monitoring the fluorescence change of NADH upon mixing the two compounds in the stopped-flow spectrofluorometer. The fluorescence of NADH increases upon binding to the enzyme, and the change appears to be monophasic (Figure 1, upper panel). Traces of the fluorescence changes were fitted to eq 2 to obtain observed rate constants (k_{obs}) that were used for calculating the second-order rate constant for binding (k_{on}) of NADH.

$$F = A(1 - e^{-k_{obs}t}) + C \quad (2)$$

$$k_{obs} = k_{on}[LuxG] + k_{off} \quad (3)$$

The observed rate constants (k_{obs}, for concentrations ≥ 26 μM luxG) for the binding reaction are linearly dependent on the concentrations of LuxG (eq 3, Figure 1, middle panel), indicating that the binding is a one-step process with a k_{on} (slope of the plot) of $5.1 \times 10^4\ M^{-1}\ s^{-1}$ and k_{off} (intercept of the plot) of $1.3\ s^{-1}$. The dissociation constant (K_d) could also be determined from the amplitudes of the fluorescence changes of the stopped-flow data as shown in Figure 1, lower panel. These values, which varied according to the LuxG concentrations (Figure 1), were used for calculating the dissociation constant (K_d) of the LuxG:NADH complex according to eqs 4 and 5. The value obtained, 25 ± 4 μM (Figure 1, lower panel), agrees well with the K_d value calculated from the kinetic constants (Figure 1, $k_{off}/k_{on} = 25 \pm 2$ μM).

$$\Delta F = \frac{\Delta F_{max} P_{free}}{K_d + P_{free}} \quad (4)$$

$$P_{free} = P_{tot} - L_{tot}\left(\frac{\Delta F}{\Delta F_{max}}\right) \quad (5)$$

In eqs 4 and 5, ΔF is the fluorescence change observed at each concentration of LuxG, while ΔF_{max} is the maximum change at the saturating concentration of LuxG. P_{free} is the concentration of LuxG in free form, while P_{tot} is the total concentration of LuxG in each titration. K_d is the dissociation constant of the protein−ligand complex.

The stoichiometry of NADH binding to LuxG was investigated by an equilibrium binding method. Free NADH was separated from a solution containing LuxG (28 μM) and NADH (100 μM) using Centriprep YM-10 ultrafiltration tubes. The bound NADH concentration was calculated by subtracting the free from the total NADH concentration. Results showed that NADH binds to LuxG with the ratio of 1:1 (NADH:subunit).

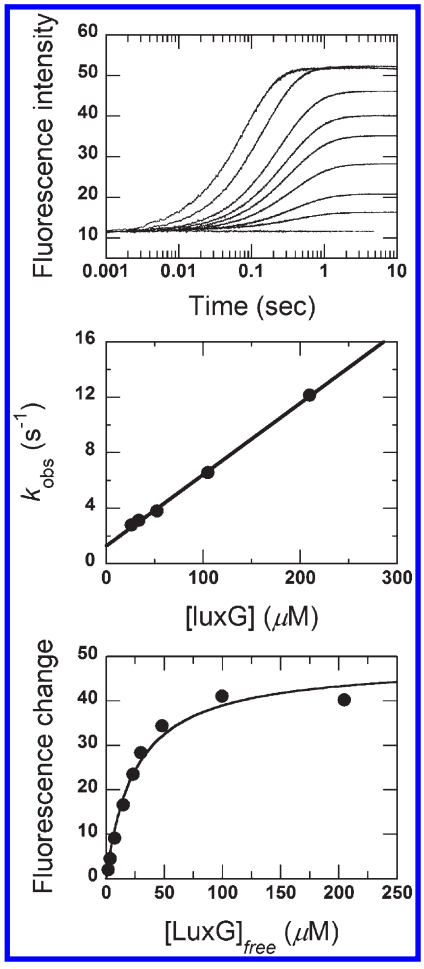

FIGURE 1: Upper panel: Kinetics of binding of LuxG to NADH. NADH (5.25 μM final) was mixed with LuxG at concentrations after mixing of 0, 4.2, 8.4, 17, 26, 34, 52, 105, and 210 μM (the lower to upper traces). The fluorescence of NADH was monitored using excitation at 340 nm and detecting emission at >400 nm (the upper panel). Middle panel: This plot shows that the observed rate constants from the kinetic traces are linearly dependent on the LuxG concentrations, indicating a one-step binding process with k_{on} (slope) of $5.1 \times 10^4\ M^{-1}\ s^{-1}$ and k_{off} (intercept) of $1.3\ s^{-1}$ (only LuxG concentrations of 26 μM and higher, where pseudo-first-order conditions hold, were used in the analysis.) Lower panel: This plot shows the relationship of the total observed fluorescence changes at each concentration of LuxG due to binding of NADH as shown in the upper panel. Values for $[LuxG]_{free}$ were calculated according to eqs 4 and 5. The fluorescence change of NADH was hyperbolically dependent on the concentration of LuxG added. The concentration of free LuxG giving a half-saturation value of the plot represents the K_d value of the binding of NADH to LuxG (25 ± 4 μM).

Binding of FMN to LuxG. The binding of FMN to LuxG was investigated by monitoring spectroscopically a titration of FMN with LuxG using changes in the absorbance or fluorescence signals. It was found that no changes in the signal occurred other than those due to dilution of the FMN solution. The ultrafiltration approach (described in Materials and Methods) was used to determine the amount of free FMN at each concentration of protein. The fluorescence emission intensity with an excitation wavelength at 450 nm was used to quantify the free FMN. The results showed that free FMN concentrations did

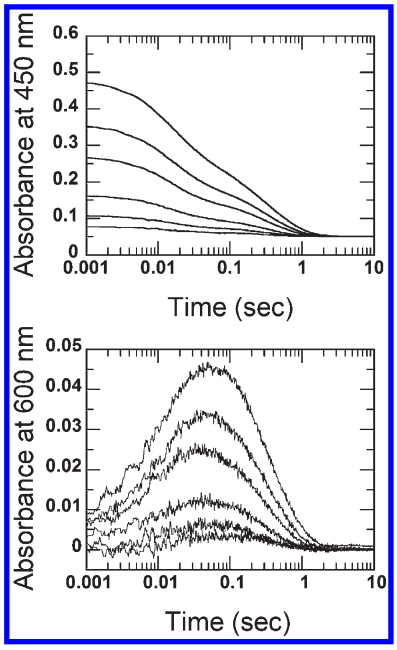

FIGURE 2: Kinetic traces for the reduction of FMN by NADH catalyzed by LuxG. A solution of LuxG (50 μM, final concentration of monomer) and NADH (300 μM, final concentration) was mixed with various concentrations of FMN (after mixing concentrations were 2.5, 5, 10, 20, 30, and 40 μM) under anaerobic conditions. The reactions were monitored at 450 nm (upper panel) and 600 nm (lower panel) using the stopped-flow spectrophotometer. Upper to lower traces represent the reactions from higher to lower concentrations of FMN. Data were fitted with two exponentials: the first reduction phase (A_{450} decrease and A_{600} increase) with k_{obs} of 68 ± 6 s^{-1} and the second reduction phase (A_{450} decrease and A_{600} decrease) with k_{obs} of 2.8 ± 0.2 s^{-1}.

not change upon increasing the LuxG concentration, implying that at any practical concentrations FMN does not bind to LuxG. Thus, all of the binding results indicate that NADH binds to the enzyme as the first substrate prior to FMN binding.

Kinetics of the LuxG-Catalyzed Reduction of FMN by NADH. A solution containing LuxG and NADH was mixed with equal volumes of solutions containing various concentrations of FMN under anaerobic conditions in the stopped-flow spectrophotometer. The reduction of FMN was monitored by the absorbance changes at 450 nm, while pyridine nucleotide−flavin charge-transfer intermediates were monitored by absorbance changes at 600 nm. Reactions of flavoproteins with reduced pyridine nucleotides often result in formation of two types of charge-transfer complexes. First, a complex called CT-1 (i.e., NADH−FMN) forms, and subsequently a hydride transfer results in CT-2 (i.e., $FMNH^-$:NAD^+). In the reactions with NADH, two phases due to reduction of FMN were observed at 450 nm, and each accounted for ~50% of the total absorbance change (Figure 2, upper panel). The fractions in the two phases remained constant over a wide range of FMN concentrations (all less than that of LuxG), suggesting that there is negative cooperativity resulting in half-sites reactivity. Moreover, because the concentrations of FMN were lower than that of LuxG in all cases, but both phases were always apparent with equal amplitudes, it can be concluded that the second FMN binds to the LuxG dimer faster than the first. Otherwise, at these low concentrations of FMN one would expect the FMN to distribute such that most of the species would be dimers with a single bound FMN, and only a single phase would be seen. Thus, paradoxically, binding of FMN to the LuxG:NADH complex appears to be positively cooperative, although after binding, the actual reduction reactions exhibit negative cooperativity. The phases are clearly kinetically separated, with the ratio of k_{obs1}/k_{obs2} being ~20. The observed rate constants (k_{obs}) for the first and second phases are 68 ± 6 s^{-1} and 2.8 ± 0.2 s^{-1}, respectively, and did not depend on the concentrations of FMN used (Figure 2).

The absorbance traces observed at 600 nm are also composed of two phases, with the first phase characterized by an absorbance increase that is complete by ~50 ms, while the second phase is characterized by an absorbance decrease that is complete by ~2 s (Figure 2, lower panel). The increase of absorbance at 600 nm in the first phase occurs at the same rate as the reduction observed at 450 nm (68 ± 6 s^{-1}). It is therefore assigned as formation of the second charge-transfer complex on the first reacting subunit (CT-2, FMN_{red}:NAD^+) (see the next section). This is followed by a decrease in absorbance at 600 nm at the same rate as the slower phase observed at 450 nm (2.8 ± 0.2 s^{-1}). Thus, decay of the charge-transfer complex coincides with the slower phase of reduction, suggesting that the FMN on the second subunit does not become reduced until the CT interaction on the first has dissipated, probably by the dissociation of NAD^+. The observed rate constants (k_{obs}) at 600 nm for both phases are independent of the concentration of FMN and correlate well with the k_{obs} values obtained at 450 nm. The amplitudes of the kinetics traces at 600 nm increased with FMN concentration, which is consistent with increased occupancy of the active sites of both subunits by flavin.

Because the reactions monitored were not under pseudo-first-order conditions, kinetic analysis to determine an accurate K_d for the binding of FMN to the LuxG:NADH complex was not straightforward. Nevertheless, because the observed rate constants of all phases were the same at all FMN concentrations used, it can be estimated that the K_d is considerably less than 2.5 μM (the lowest concentration of FMN used), and k_{red} (rate constant for the flavin reduction) is approximately 68 s^{-1}. Overall from these results, the biphasic flavin reduction with similar amplitudes in both phases is consistent with a half-sites kinetic model for the reaction of LuxG that involves sequential reduction of FMN bound to the two subunits.

Spectra occurring at particular times during the reaction of 50 μM LuxG, 20 μM FMN, and 300 μM NADH (under the same conditions as in Figure 2) could be extracted from kinetic traces recorded at a series of wavelengths. Figure 3 shows spectra obtained at 0.002 s (approximate instrument dead time), at 0.050 s (after the first phase), and at 10 s (when the reaction was complete). These spectra show that only half of the total FMN was reduced by the end of the first phase (during the first 0.05 s, open circle spectrum). The other half, which was still in the oxidized form and showed a resolved shoulder near 450 nm, is more typical for an enzyme-bound flavin than is the starting spectrum. We also note that the spectra at 2 ms and at 0.05 s are red shifted to ~450 nm because of binding to LuxG. A charge-transfer species with a broad absorption band between 500 and 700 nm had fully formed by the end of the first phase. Overall, these results are consistent with the notion that after the first phase (68 s^{-1}) only 50% of the LuxG-bound FMN has been reduced by NADH and that this process occurred on only one subunit of the dimeric enzyme. The FMN in the other subunit of LuxG appears to be reduced only after both NAD^+ and possibly $FMNH^-$ are released from the first subunit at ~2.8 s^{-1}. Thus, although the actual reduction of FMN on the second subunit could be as rapid (e.g., 68 s^{-1}) as on the first subunit, the overall

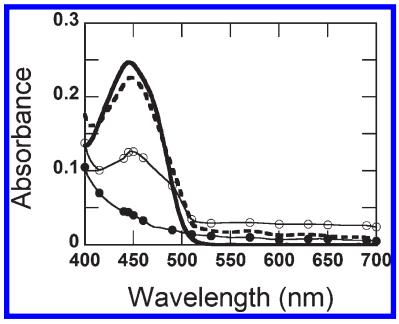

FIGURE 3: Absorption spectra observed during the reduction of FMN by NADH catalyzed by LuxG. A solution of LuxG (50 μM, final concentration) and NADH (300 μM, final concentration) was mixed with FMN (20 μM after mixing) under anaerobic conditions. The displayed spectra at various times are extracted from the kinetic traces recorded at various wavelengths, ranging from 390 to 700 nm. The spectra are as follows: thick solid line (initial 20 μM FMN), dashed line (from the reaction time of 2 ms), open circles (from the reaction time of 50 ms), and closed circles (from the reaction time of 10 s).

Scheme 1: Reaction of LuxG Displays Half-Sites Reactivity[a]

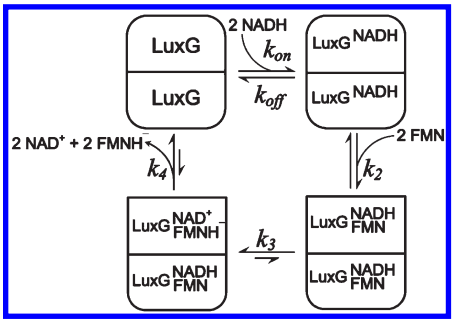

[a]The kinetic constants, k_x, refer to those in Table 1. The first step of the reaction is the binding of two NADH to form the LuxG:NADH dimer complex. Two FMN then bind with positive cooperativity in the second step. Flavin reduction on one subunit in LuxG occurs rapidly (68 s^{-1}). The reduction of the second FMN is apparently limited by the release of the NAD^+ and/or $FMNH^-$ at the first site at ~2.8 s^{-1}. Upon reduction, $FMNH^-$ and NAD^+ from the second site are released rapidly so that the last phase of flavin reduction and the loss of the charge-transfer spectra derived from the first site appear as a single exponential process. Because of the unusual kinetics, no charge-transfer species are observed during the reduction of the second FMN.

reaction rate in the second subunit appears to be limited by product release from the first subunit. Scheme 1 describes the half-sites reactivity hypothesis for LuxG. According to this model, both subunits are active, but flavin reduction occurs with significant negative cooperativity. This model also predicts that the overall rate of LuxG reaction under anaerobic condition is limited by a rate constant of ~2.8 s^{-1}.

Kinetics of the LuxG-Catalyzed FMN Reduction by 4(R)-NADD. Experiments similar to those just described were performed using 4(*R*)-NADD instead of NADH. In these reactions, rate constants of any steps involving hydride transfer (flavin reduction) should be affected significantly due to primary kinetic isotope effects. Comparison of the kinetic traces recorded at 450, 490, and 700 nm (Figure 4) that were due to flavin reduction using 4(*R*)-NADD and NADH helped to identify steps involved with flavin reduction and formation of charge-transfer complexes. Kinetic traces of the reaction with NADD clearly reveal an extra initial phase in addition to the kinetic phases observed using NADH (Figure 4). This initial phase can be

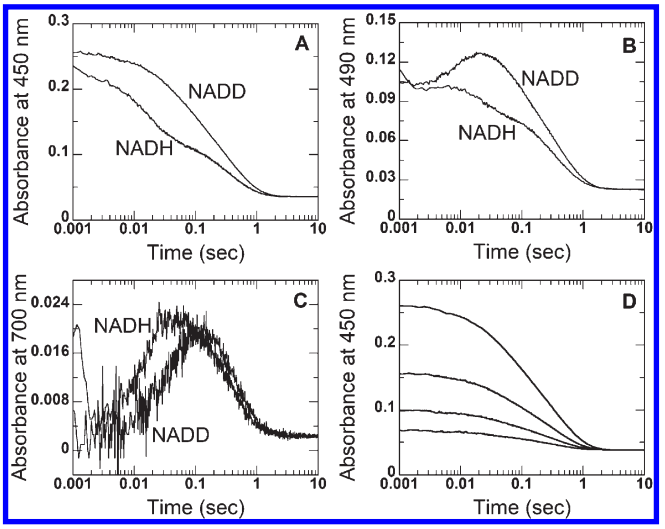

FIGURE 4: Kinetic traces of the reduction of FMN by NADH or 4(*R*)-NADD catalyzed by LuxG. A solution of LuxG (50 μM, final concentration) and NADH or 4(*R*)-NADD (300 μM, final concentration) was mixed with a solution of FMN (20 uM after mixing) under anaerobic conditions. The reaction was monitored using the stopped-flow spectrophotometer at (A) 450 nm, (B) 490 nm, and (C) 700 nm. For the reaction with NADD, data were fitted with three exponentials with k_{obs} of the first phase of 93 s^{-1}, k_{obs} of the second phase of 17.5 s^{-1}, and k_{obs} of the third phase of 2.6 s^{-1}. (D) The same solution of LuxG and NADD was mixed with various concentrations of FMN (2.5, 5, 10, and 20 μM after mixing) in the same buffer. The absorbance values at 450 nm vs time are plotted. The lower to upper traces represent the lower to higher concentrations of FMN.

observed as a small increase in absorbance at 490 nm (~0.03 A) that is likely due to formation of the first charge transfer species (CT-1, FMN_{ox}:NADH). This phase is followed by a phase with large absorbance decreases between 490 and 450 nm and a small absorbance increase at 700 nm, indicating reduction of FMN with concurrent formation of the second charge-transfer species (CT-2, FMN_{red}:NAD^+). During the third phase, all wavelengths show absorbance decreases due to the reduction of the second FMN and dissociation of the NAD^+ (or conformational change that dissipates the CT-2 interaction).

The kinetic traces observed at all wavelengths in the NADD reaction (using 300 μM NADD) could be fitted with three exponentials: k_{obs1} of ~93 s^{-1}, k_{obs2} of ~17.5 s^{-1}, and k_{obs3} of ~2.6 s^{-1}. Thus, at this concentration of NADD the CT-1 intermediate forms at a rate of 93 s^{-1}. The small increase in absorbance at 490 nm was also present when using NADH but was not as apparent because the ensuing reduction step was fast and involved a large decrease in absorbance. The measured value of 68 s^{-1} for k_{obs2} when using NADH may actually be slightly underestimated because the preceding 93 s^{-1} step to form CT-1 (when using 300 μM NADH) partially masks it. In general, the ratio of k_{obs1}/k_{obs2} should be greater than 3 to allow two consecutive exponentials to be unambiguously identified (*24*). When using NADD, the CT-1 intermediate can be easily observed because the subsequent reduction (deuteride transfer) step is considerably slower (Figure 4B). As also seen with NADH, the reduction phase observed in the NADD reaction occurred concomitantly with the formation of CT-2 as shown in the kinetic traces at 450 and 700 nm. The primary kinetic isotope effect (^Dk) for the reduction step is ≥3.9 because the true reduction rate with NADH may be greater than 68 s^{-1} as mentioned above. These data confirm that the second phase is indeed the hydride transfer step. The kinetic isotope effect is also

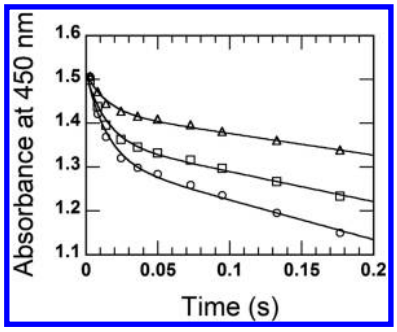

FIGURE 5: Turnover kinetics showing the burst phase of the LuxG reaction. Kinetics of the burst phase of the LuxG reaction were obtained by monitoring the absorbance at 450 nm. Solutions of LuxG (final concentrations of 20 μM (triangle), 30 μM (square), 40 μM (circle)) premixed with NADH (300 μM, final concentration) were mixed against FMN (125 μM, final concentration, starting value of A_{450} = 1.53) using the stopped-flow spectrophotometer. The lines are fits to the data according to eq 1. Details of the analysis are described in the text. The results indicate that the ratios of FMN used during the first turnover to the LuxG−NADH complex are 0.45, 0.53, and 0.52 at LuxG concentrations of 20, 30, and 30 μM, respectively, indicating a ratio of ~1 mol of FMN/2 mol of LuxG.

consistent with the model in Scheme 1. Because the release of NAD^+ (2.8 s^{-1}) limits the reduction rate, no isotope effect was observed for the reduction of the FMN on the second subunit.

Burst Kinetics of LuxG. The half-sites reactivity model described in Scheme 1 predicts that when a solution of LuxG and excess NADH is mixed with a solution containing an excess of FMN over LuxG, there will be a burst of flavin reduction that should be approximately 50% of the concentration of LuxG:NADH. This would be followed by a steady-state production of $FMNH^-$ that is equivalent to the turnover number under those conditions. A solution of the LuxG:NADH complex was mixed with a solution of FMN under anaerobic conditions in the stopped-flow apparatus, and the reaction was followed at 450 nm (Figure 5). A burst followed by a steady-state rate of reduction was observed. The magnitude of the burst and the steady-state rate were both dependent on the concentration of LuxG. Kinetic traces in Figure 5 can be fitted using eq 1 (an exponential decrease plus a linear phase) with k_{red} equal to 68 s^{-1} (Figure 5).

When LuxG (20 μM) was used, the concentration of the LuxG:NADH complex could be calculated from the K_d of 25 μM to be 18.4 μM. Analysis of this trace (the top trace in Figure 5) yielded A_0 of 0.088 and a slope for the linear part of 0.49 A/s. These data indicated that 8.4 ± 0.5 μM FMN (46% of the LuxG:NADH complex) was reduced during the burst phase and the turnover number for the steady-state phase was 2.5 s^{-1}. For the reactions of 30 and 40 μM LuxG (middle and bottom traces), the same analysis indicated that 53% and 52% of the LuxG:NADH complex were reduced during the burst phase, respectively, and both concentrations of LuxG showed turnover numbers of 2.35 s^{-1} (Figure 5). Taken together, the data in Figure 5 indicate that the burst corresponds to the reduction of only about half of the bound FMN per LuxG and is consistent with the model described in Scheme 1, strongly suggesting that LuxG functions via a half-sites reactivity model.

DISCUSSION

Our previous steady-state kinetic data showed that the reaction of LuxG from *P. leiognathi* follows a ternary complex mechanism in which both substrates (NADH and FMN) bind to the enzyme before the reduction proceeds to form $FMNH^-$ and NAD^+ (*10*). In this report, details of the reaction mechanism of LuxG were further investigated using transient kinetic methods at 4 °C. Our data suggest that substrate binding in LuxG is ordered and sequential with NADH being the first substrate that binds to the active site, followed by FMN. This is consistent with the finding that NADH can bind to LuxG, but FMN binding could not be detected unless NADH was already bound (Figures 1 and 3). This substrate binding sequence is similar to that of *E. coli* Fre, which was investigated with steady-state kinetic methods (*18*). Mixing FMN with the NADD:LuxG complex results in formation of the first charge-transfer species (CT-1, FMN_{ox}:NADD) as evidenced by the absorbance increase at ~490 nm that occurs before the hydride transfer occurs (Figure 4B). Our data here show that LuxG is a flavin reductase catalyzing the transfer of a pro-(*R*)-hydride of NADH to FMN_{ox}, similar to the reactions of *E. coli* Fre (*19*) and phthalate dioxygenase reductase (PDR) from *Pseudomonas cepacia* (*22*, *25*). Both *E. coli* Fre and PDR are members of the FNR family (*26*). A primary deuterium isotope effect of ≥3.9 was detected when 4(*R*)-NADD was used instead of NADH, allowing us to unambiguously identify steps involved with FMN reduction. FMN is reduced by NADH with a k_{obs} of ≥68 s^{-1}, resulting in formation of the second charge-transfer species (CT-2, FMN_{red}:NAD^+), which absorbs more strongly at longer wavelengths (~700 nm) than CT-1. These two charge-transfer intermediates, CT-1 and CT-2, have also been observed and show similar spectral characteristics in the reactions of *E. coli* Fre (*26*), *P. cepacia* PDR (*22*, *25*), and spinach FNR (*28*, *29*). After the FMN is reduced, the products NAD^+ and, presumably, $FMNH^-$ are released from LuxG with a k_{obs} of 2.8 s^{-1}. Given the similarities to *E. coli* Fre and the likely symmetry for binding substrates, we presume that the product $FMNH^-$ is released before NAD^+, although no experiments were explicitly carried out to test this idea.

Our transient kinetic data reported here indicate that LuxG catalyzes the reaction using a half-sites reactivity model (Scheme 1). According to this model, FMN binds to both subunits of the LuxG:NADH complex, but only one of the two FMNs becomes reduced in the first reduction phase (out to ~0.05 s) (Figures 2 and 3), while FMN bound to the other subunit remains in the oxidized form. The model in Scheme 1 is consistent with the burst kinetics data showing that ~50% of the LuxG:NADH complex is reduced during the burst phase (Figure 5). The model in Scheme 1 also implies that both active sites of LuxG are active and that under anaerobic conditions the overall turnover rate of LuxG is limited by the rate constant of 2.8 s^{-1}. Analysis of the traces in Figure 5 yielded the turnover number of 2.4 s^{-1}, which is consistent with the model in Scheme 1. According to the previous report (*10*), the turnover number from the steady-state kinetics under aerobic conditions is ~1.7 s^{-1}. This result indicates in these experiments, in addition to the last step (2.8 s^{-1}) in Scheme 1, the reaction of reduced LuxG with oxygen may also affect the overall turnover rate of LuxG. Alternatively, the enzyme used in the steady-state experiments reported in ref *10* may not have been fully active, which would give a lower apparent turnover number.

Based on their sequence similarity and kinetic mechanisms, LuxG is closely related to *E. coli* Fre (*10*). However, the half-sites reactivity of LuxG is quite different from *E. coli* Fre. Although *E. coli* Fre and LuxG have considerable homology in their amino acid sequences, Fre is a monomeric enzyme while LuxG is a

dimer. Therefore, the half-sites reactivity mechanism is not possible in Fre.

This half-sites phenomenon has been observed in a few enzymes such as acetoacetate decarboxylase, *E. coli* aspartate transcarbamylase, and yeast alcohol dehydrogenase (*30*). However, no flavin reductases have been reported previously with this property. Half-sites reactivity can be caused by three main factors (*30*): (1) nonidentical subunits, (2) steric hindrance of the active sites (if the active sites of two subunits are near the axis of symmetry, the binding of a ligand at one site may generate steric or electrostatic constraints that inhibit the ligand binding at the other site), and (3) induction of change in protein quaternary structure during catalysis. In the case of LuxG the first explanation can be ruled out since each subunit of LuxG is identical and encoded by a single gene, but either the second or third explanation is possible. Although the binding of FMN to LuxG could not be observed using ultrafiltration or spectroscopic measurements, transient kinetics indicates that FMN binds tightly and rapidly to the LuxG:NADH complex (Figure 2). It indicates that LuxG must be in complex with NADH for FMN to bind, possibly because NADH induces a conformational change that promotes the binding of FMN. It is possible that the binding site for FMN is at the dimeric interface of the LuxG:NADH complex, in which case the half-sites activity could arise from steric hindrance that prevents access of NADH to the FMN in the second subunit until after the reduction of FMN in the first subunit is complete. Future investigations on the structure of LuxG are needed to identify factors causing the half-sites reactivity in this enzyme. As of now, there is no definitive explanation about the biological significance of enzymes with the half-sites reactivity.

Other flavin reductases from luminous bacteria that have been investigated are *V. fischeri* FRaseI (*31*) and *V. harveyi* FRP (*32*). Amino acid sequences and catalytic properties of these enzymes are significantly different from those of LuxG (*10*). FRaseI and FRP are flavoproteins containing FMN as cofactors, while LuxG binds FMN as a substrate rather than a prosthetic group. Steady-state kinetic data obtained with FRaseI and FRP indicate that they follow a ping-pong-type mechanism (*31*, *32*), which is different from the ternary complex mechanism utilized by LuxG (*10*). Pre-steady-state kinetics of FRaseI and FRP have not been reported. Although FRaseI and FRP can be used *in vitro* for providing reduced FMNH to bacterial luciferase, it can be concluded that the flavin reductase selected over the course of evolution to function in generating reduced FMN for bacterial luciferase is LuxG, because the genes of LuxG and LuxAB are encoded in the same operon (*10*, *33*). Therefore, pre-steady-state kinetic data reported here will be instrumental in future investigations on the $FMNH^-$ transfer from LuxG to bacterial luciferase.

In the two-component flavin-dependent enzyme, *p*-hydroxyphenylacetate hydroxylase from *Acinetobacter baumannii*, the flavin reductase component (C_1) shows properties that coordinate its activity with that of the oxygenase component (C_2) (*21*, *34*−*36*). Thus, HPA (the substrate for C_2) allosterically increases the affinity of C_1 to NADH, the rate of flavin reduction, and the rates of NAD^+ and $FMNH^-$ dissociation (*21*), thereby enabling the rapid delivery of $FMNH^-$ to C_2 to carry out the hydroxylation. $FMNH^-$ is transferred from C_1 to the C_2 component via simple diffusion (*37*). In contrast, when adding dodecanal, an aldehyde substrate of LuxAB, to the assay reaction, we found that the activity of LuxG was not affected (data not shown). In the oxygenase system involved with actinorhodin biosynthesis (ActVA−ActVB), a stable charge-transfer complex of NAD^+ and reduced FMN forms during catalysis (*37*), and the dissociation of this complex, which is controlled by the concentration NAD^+, limits the overall rate of the ActVA−ActVB reaction (*38*). This characteristic enables NAD^+ to act as a regulatory component in this two-component system. A similar charge-transfer complex (CT-2) was also observed in the LuxG reaction, but it was not as stable as that found with ActVB, suggesting that a different means is required to control the LuxG−LuxAB reaction system. Recently, transient kinetics of SsuE, a flavin reductase (that like LuxG does not use flavin as a cofactor) in the alkanesulfonate monooxygenase system, has been reported (*39*). The overall reaction mechanism of SsuE is similar to that of LuxG in which both substrates (NADPH and FMN) bind to the enzyme to form a CT-1 (FMN_{ox}:NADH) intermediate. Then, reduction of flavin occurs concurrently with formation of CT-2 (FMN_{red}:NAD^+) before the products ($NADP^+$ and $FMNH^-$) dissociate from the enzyme (*39*).

Although the discovery of two-component flavin-dependent monooxygenase systems continues to expand, only a few flavin reductase components have been characterized in detail. This work has elucidated the kinetic mechanism and identified an intermediate of the reaction of LuxG, a flavin reductase of the bacterial luciferase system. The catalysis of LuxG has been shown to proceed according to an ordered-sequential mechanism. Overall, the reaction mechanism and the intermediates observed are quite similar to those of other enzymes in the FNR family, including *E. coli* Fre, but the unique feature of LuxG is the half-sites reactivity that has never been reported in other flavin reductases.

ACKNOWLEDGMENT

We thank Barrie Entsch, University of New England, NSW, Australia, for critical reading of the manuscript.

REFERENCES

1. Fontecave, M., Coves, J., and Pierre, J. L. (1994) Ferric reductases or flavin reductases? *Biometals*. *7*, 3–8.
2. Hasan, N., and Nester, E. W. (1978) Purification and characterization of NADPH-dependent flavin reductase. An enzyme required for the activation of chorismate synthase in *Bacillus subtilis*. *J. Biol. Chem*. *253*, 4987–4992.
3. Fontecave, M., Eliasson, R., and Reichard, P. (1987) NAD(P)H: flavin oxidoreductase of *Escherichia coli*. A ferric iron reductase participating in the generation of the free radical of ribonucleotide reductase. *J. Biol. Chem*. *262*, 12325–12331.
4. Ballou, D. P., Entsch, B., and Cole, L. J. (2005) Dynamics involved in catalysis by single-component and two-component flavin-dependent aromatic hydroxylases. *Biochem. Biophys. Res. Commun*. *338*, 590–598.
5. Van Berkel, W. J., Kamerbeek, N. M., and Fraaije, M. W. (2006) Flavoprotein monooxygenases, a diverse class of oxidative biocatalysis. *J. Biotechnol*. *124*, 760–789.
6. Ellis, H. R. (2010) The FMN-dependent two-component monooxygenase systems. *Arch. Biochem. Biophys*. *497*, 1–12.
7. Chaiyen, P., Suadee, C., and Wilairat, P. (2001) A novel two-protein component flavoprotein hydroxylase. *Eur. J. Biochem*. *268*, 5550–5561.
8. Arunachalam, U., Massey, V., and Miller, S. M. (1994) Mechanism of *p*-hydroxyphenylacetate-3-hydroxylase. A two-protein enzyme. *J. Biol. Chem*. *269*, 150–155.
9. Valton, J., Filisetti, L., Fontecave, M., and Niviere, V. (2004) A two-component flavin-dependent monooxygenase involved in actinorhodin biosynthesis in *Streptomyces coelicolor*. *J. Biol. Chem*. *279*, 44362–44369.

10. Nijvipakul, S., Wongratana, J., Suadee, C., Entsch, B., Ballou, D. P., and Chaiyen, P. (2008) LuxG is a functioning flavin reductase for bacterial luminescence. *J. Bacteriol. 190*, 1531–1538.
11. Suadee, C., Nijvipakul, S., Svasti, J., Entsch, B., Ballou, D. P., and Chaiyen, P. (2007) Luciferase from *Vibrio campbellii* is more thermostable and binds reduced FMN better than its homologues. *J. Biochem. 142*, 539–552.
12. Campbell, Z. T., and Baldwin, T. O. (2009) Fre is the major flavin reductase supporting bioluminescence from *Vibrio harveyi* luciferase in *Escherichia coli*. *J. Biol. Chem. 284*, 8322–8328.
13. Zenno, S., Saigo, K., Kanoh, H., and Inouye, S. (1994) Identification of the gene encoding the major NAD(P)H-flavin oxidoreductase of the bioluminescent bacterium *Vibrio fischeri* ATCC 7744. *J. Bacteriol. 176*, 3536–3543.
14. Lei, B., Liu, M., Huang, S., and Tu, S. C. (1994) *Vibrio harveyi* NADPH-flavin oxidoreductase: cloning, sequencing and overexpression of the gene and purification and characterization of the cloned enzyme. *J. Bacteriol. 176*, 3552–3558.
15. Tu, S. C. (2001) Reduced flavin: donor and acceptor enzymes and mechanisms of channeling. *Antioxid. Redox Signal. 3*, 881–897.
16. Koike, H., Sasaki, H, Kobori, T, Zenno, S, Saigo, K, Murphy, M. E., Adman, E. T., and Tanokura, M. (1998) 1.8 Å crystal structure of the major NAD(P)H:FMN oxidoreductase of a bioluminescent bacterium, *Vibrio fischeri*: overall structure, cofactor and substrate-analog binding, and comparison with related flavoproteins. *J. Mol. Biol. 280*, 259–273.
17. Ingelman, M., Ramaswamy, S., Niviere, V., Fontecave, M., and Eklund, H. (1999) Crystal structure of NAD(P)H:flavin oxidoreductase from *Escherichia coli*. *Biochemistry. 38*, 7040–7049.
18. Fieschi, F., Niviere, V., Frier, C., Decout, J. L., and Fontecave, M. (1995) The mechanism and substrate specificity of the NADPH:flavin oxidoreductase from *Escherichia coli*. *J. Biol. Chem. 270*, 30392–30400.
19. Niviere, V., Fieschi, F., Decout, J. L., and Fontecave, M. (1999) The NAD(P)H:flavin oxidoreductase from *Escherichia coli*. Evidence for a new mode of binding for reduced pyridine nucleotides. *J. Biol. Chem. 274*, 18252–18260.
20. Zenno, S., and Saigo, K. (1994) Identification of the genes encoding NAD(P)H-flavin oxidoreductases that are similar in sequence to *Escherichia coli* Fre in four species of luminous bacteria: *Photorhabdus luminescens*, *Vibrio fischeri*, *Vibrio harveyi*, and *Vibrio orientalis*. *J. Bacteriol. 176*, 3544–3551.
21. Sucharitakul, J., Chaiyen, P., Entsch, B., and Ballou, D. P. (2005) The reductase of *p*-hydroxyphenylacetate 3-hydroxylase from *Acinetobacter baumannii* requires *p*-hydroxyphenylacetate for effective catalysis. *Biochemistry 44*, 10434–10442.
22. Gassner, G., Wang, L., Batie, C., and Ballou, D. P. (1994) Reaction of phthalate dioxygenase reductase with NADH and NAD: kinetic and spectral characterization of intermediates. *Biochemistry 33*, 12184–12193.
23. Patil, P. V., and Ballou, D. P. (2000) The use of photocatechuate dioxygenase for maintaining anaerobic conditions in biochemical experiments. *Anal. Biochem. 286*, 187–192.
24. Hiromi, K. (1979) Analysis of Fast Enzyme Reactions: Transient Kinetics, Kinetics of Fast Enzyme Reactions: Theory and Practice, pp 187−244, Kodansha Ltd., Tokyo.
25. Gassner, G. T., and Ballou, D. P. (1995) Preparation and characterization of a truncated form of phthalate dioxygenase reductase that lacks an iron-sulfur domain. *Biochemistry 34*, 13460–13471.
26. Niviere, V., Vanoni, M. A., Zanetti, G., and Fontecave, M. (1998) Reaction of the NAD(P)H:flavin oxidoreductase from *Escherichia coli* with NADPH and riboflavin: identification of intermediates. *Biochemistry 37*, 11879–11887.
27. Karplus, P. A., and Bruns, C. M. (1994) Structure-function relations for ferredoxin reductase. *J. Bioenerg. Biomembr. 26*, 89–99.
28. Batie, C. J., and Kamin, H. (1984) Electron transfer by ferredoxin: $NADP^+$ reductase. Rapid-reaction evidence for participation of a ternary complex. *J. Biol. Chem. 259*, 11976–11985.
29. Batie, C. J., and Kamin, H. (1986) Association of ferredoxin-$NADP^+$ reductase with NADP(H) specificity and oxidation-reduction properties. *J. Biol. Chem. 261*, 11214–11223.
30. Seydoux, F., Malhotra, O. P., and Bernhard, S. A. (1974) Half-site reactivity. *CRC Crit. Rev. Biochem. 2*, 227–257.
31. Inouye, S. (1994) NAD(P)H-flavin oxidoreductase from the bioluminescent bacterium, *Vibrio fischeri* ATCC 7744, is a flavoprotein. *FEBS Lett. 347*, 163–168.
32. Lei, B., and Tu, S. C. (1998) Mechanism of reduced flavin transfer from *Vibrio harveyi* NADPH-FMN oxidoreductase to luciferase. *Biochemistry 37*, 14623–14629.
33. Meighen, E. A. (1994) Genetics of bacterial bioluminescence. *Annu. Rev. Genet. 28*, 117–139.
34. Thotsaporn, K., Sucharitakul, J., Wongratana, J., Suadee, C., and Chaiyen, P. (2004) Cloning and expression of *p*-hydroxyphenylacetate 3-hydroxylase from *Acinetobacter baumannii*: evidence of the divergence of enzymes in the class of two-protein component aromatic hydroxylases. *Biochim. Biophys. Acta 1680*, 60–66.
35. Sucharitakul, J., Chaiyen, P., Entsch, B., and Ballou, D. P. (2006) Kinetic mechanisms of the oxygenase from a two-component enzyme, p-hydroxyphenylacetate 3-hydroxylase from *Acinetobacter baumannii*. *J. Biol. Chem. 281*, 17044–17053.
36. Sucharitakul, J., Phongsak, T., Entsch, B., Svasti, J., Chaiyen, P., and Ballou, D. P. (2007) Kinetics of a two-component *p*-hydroxyphenylacetate hydroxylase explain how reduced flavin is transferred from the reductase to the oxygenase. *Biochemistry 46*, 8611–8623.
37. Filisetti, L., Fontecave, M., and Niviere, V. (2003) Mechanism and substrate specificity of the flavin reductase ActVB from *Streptomyces coelicolor*. *J. Biol. Chem. 278*, 296–303.
38. Valton, J., Mathevon, C., Fontecave, M., Niviere, V., and Ballou, D. P. (2008) The two-component FMN-dependent monooxygenase ActVA-ActVB from *Streptomyces coelicolor*: mechanism and regulation. *J. Biol. Chem. 283*, 10287–10296.
39. Gao, B., and Ellis, H. R. (2007) Mechanism of flavin reduction in the alkanesulfonate monooxygenase system. *Biochim. Biophys. Acta 1774*, 359–367.